Solvent effect and device optimization of diketopyrrolopyrrole and carbazole copolymer based solar cells

Aïch, Réda Badrou; Zou, Yingping; Leclerc, Mario; Tao, Ye

Publisher's version / Version de l'éditeur:
https://doi.org/10.1016/j.orgel.2010.03.004
Organic Electronics, 11, 6, pp. 1053-1058, 2010-06-01

Organic Electronics 11 (2010) 1053–1058

Contents lists available at ScienceDirect

Organic Electronics

journal homepage: www.elsevier.com/locate/orgel

Solvent effect and device optimization of diketopyrrolopyrrole and carbazole copolymer based solar cells

Réda Badrou Aïch [a,b], Yingping Zou [b], Mario Leclerc [b], Ye Tao [a,*]

[a] Institute for Microstructural Sciences, National Research Council of Canada, Ottawa, ON, Canada K1A 0R6
[b] Département de Chimie, Université Laval, Québec City, QC, Canada G1K 7P4

ARTICLE INFO

Article history:
Received 18 November 2009
Received in revised form 3 March 2010
Accepted 6 March 2010
Available online 16 March 2010

Keywords:
Solar cells
Polymer structure
Solvent effect
Carbazole

ABSTRACT

Bulk heterojunction organic photovoltaic cells using blends of poly[*N*-9′-heptadecanyl-2,7carbazole-alt-3,6-bis(thiophen-5-yl)-2,5-dioctyl-2,5-dihydropyrrolo[3,4-]pyrrole-1,4-dione] (PCBTDPP) and [6,6]-phenyl-C61-butyric acid methyl ester ($PC_{60}BM$) or [6,6]-phenyl-C71-butyric acid methyl ester ($PC_{70}BM$) as electron donor and acceptor were fabricated and characterized. Devices made from 1,2-dichlorobenzene solution demonstrated better performance in terms of short-circuit current density, open-circuit voltage and power conversion efficiency, as compared to the devices made from chloroform and chlorobenzene solutions. By optimizing the donor/acceptor ratio and the thickness of the active layer, a power conversion efficiency of 3.2% was achieved on devices with an active device area of 1 cm^2, under 100 mW/cm^2 of simulated AM1.5 irradiation.

1. Introduction

Conjugated polymers have attracted considerable attention due to their various applications in polymer solar cells (OPVs) [1], organic field effect transistors (OFETs) [2], sensors [3], and thermoelectric devices [4], etc. In order to get efficient devices, it is necessary to tune their properties according to specific applications. For conjugated polymers used in OPVs, bandgap and charge mobilities are of crucial importance for device performance. Fullerenes and their derivatives, such as [6,6]-phenyl-C61-butyric acid methyl ester ($PC_{60}BM$) and [6,6]-phenyl-C71-butyric acid methyl ester ($PC_{70}BM$), are widely used as electron acceptor materials in these polymer solar cells due to their excellent electron transport properties. However their light absorption in the visible spectral range is relatively weak. As a result, the efforts to enhance the absorption in polymer:PCBM based solar cells are mainly focused on developing low band gap electron donor materials [5,6]. The synthesis of low band gap polymers is however, a challenge and one design strategy involved is the synthesis of copolymers comprising alternating electron-rich and electron-deficient units.

Recently, new soluble alternating poly(2,7-carbazole) derivative PCDTBT for OPV applications has shown very promising performances with a PCE of 6.1% when $PC_{70}BM$ is used as an electron-acceptor [7]. The HOMO and LUMO energy levels of this polymer are −5.45 and −3.60 eV, respectively with an electrochemical band gap of 1.85 eV which make it ideal as a donor material to work with $PC_{70}BM$. However, its hole mobility is limited, the best value obtained after annealing is 3×10^{-3} cm^2 V^{-1} s^{-1} [8]. To further increase the device efficiency, higher charge carrier mobility is desired. Along these lines, Winnewisser and coworkers [9] reported a new polymer (BBTDPP1) based on diketopyrrolopyrrole (DPP) unit which exhibits excellent ambipolar charge transport properties. The field effect hole mobility of this polymer reached 0.1 cm^2 V^{-1} s^{-1}. Enlightened by this work, we developed a new class of polymers based on the DPP and carbazole units.

The synthesis of these polymers is described elsewhere [10,11]. In this paper we report the performance of poly[N-9′-heptadecanyl-2,7-carbazole-alt-3,6-bis(thiophen-5-yl)-2,

* Corresponding author. Tel.: +1 613 998 2485.
E-mail address: Ye.Tao@nrc.ca (Y. Tao).

1566-1199/$ - see front matter Crown Copyright © 2010 Published by Elsevier B.V. All rights reserved.
doi:10.1016/j.orgel.2010.03.004

5-dioctyl-2,5-dihydropyrrolo [3,4-] pyrrole-1,4-dione] PCBTDPP, one of the best in this new class of low-bandgap polymers [11,12], in bulk heterojunction (BHJ) solar cells (OPV). Our preliminary measurements demonstrated a PCE of 1.6% from this class of materials [11]. Through further optimizations of the active layer thickness, donor/accepter loading ratio, and the selection of solvent, we have improved PCE from 1.6% to 3.2% when PCBTDPP is blended with $PC_{70}BM$.

Solar cells were fabricated using blends of PCBTDPP and $PC_{60}BM$ or $PC_{70}BM$ in different solvents and/or ratios and at various spin coating rates to reach desired active layer parameters. Precleaned indium tin oxide (ITO) coated glass substrates were used as anode. Poly(3,4-ethylenedioxythiophene):poly(sterenesulfonate) (PEDOT:PSS) was spin coated at 7000 rpm for 60s and baked for 1 h at 120 °C, as hole transport layer. After cooling down to room temperature, active layers with desired ratio and thickness were spin coated on top of the PEDOT:PSS layers. Finally, a lithium fluoride (LiF)/aluminium (Al) cathode was thermally evaporated through a shadow mask under high vacuum. The active area of the solar cell is 1 cm^2.

Scheme 1 presents the chemical structure of PCBTDPP and the energy level diagram of the BHJ solar cells.

The photovoltaic performances of those solar cells were tested under AM 1.5G irradiation of 100 mW cm^{-2}, which was calibrated using a KG5 filter covered silicon photovoltaic solar cell traceable to the National Renewable Energy Laboratory (NREL).

2. Experimental results

The thin film UV–Vis absorption spectra of pristine (PCBTDPP), $PC_{60}BM$ and $PC_{70}BM$ are shown in Fig. 1.

The pure PCBTDPP film exhibits two main absorption bands in the visible range, one in the wavelength range of 332–483 nm and the other in 502–760 nm, leaving an absorption minimum around 500 nm. As compared to $PC_{60}BM$, $PC_{70}BM$ has significantly higher absorption in the spectral range of 400–600 nm, complementary to the absorption minimum of PCBTDPP, making $PC_{70}BM$ a better electron donor material for use with PCBTDPP in BHJ solar cells.

Fig. 2 shows the external quantum efficiency (EQE) spectra of the solar cells composed of PCBTDPP blended with $PC_{60}BM$ and $PC_{70}BM$. The measured devices in each case were fabricated with the best weight ratio and thickness of active layer for $PC_{60}BM$ and $PC_{70}BM$, respectively. The EQE of $PC_{60}BM$-based device shows a maximum of 34% at 665 nm with a drastic decrease around 500 nm, which is consistent with the absorption data discussed in Fig. 1. On the other hand, the $PC_{70}BM$-based device demon-

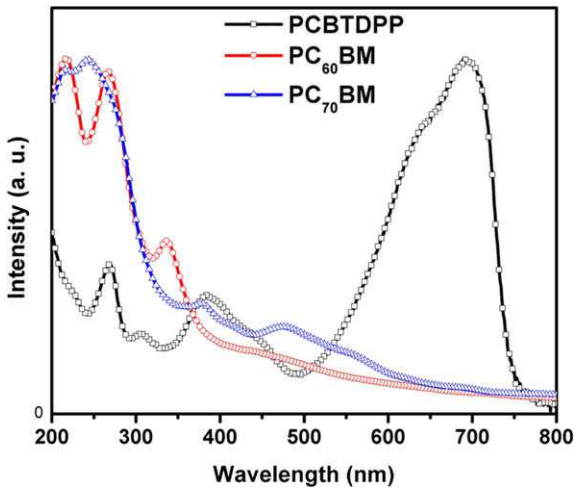

Fig. 1. UV–visible absorption spectra of PCBTDPP, $PC_{60}BM$ and $PC_{70}BM$ films.

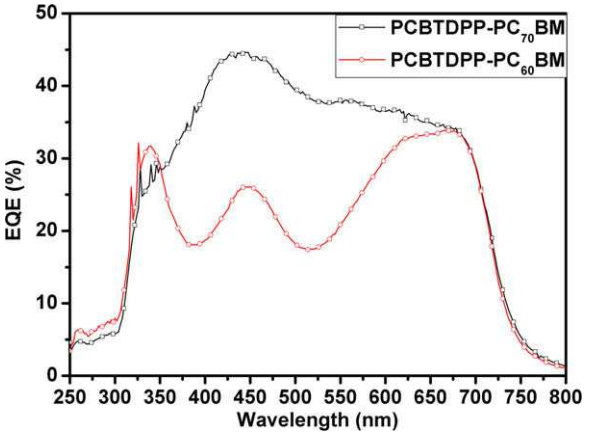

Fig. 2. EQE spectra of PCBTDPP blended with $PC_{60}BM$ (1:3) and $PC_{70}BM$ (1:3) devices.

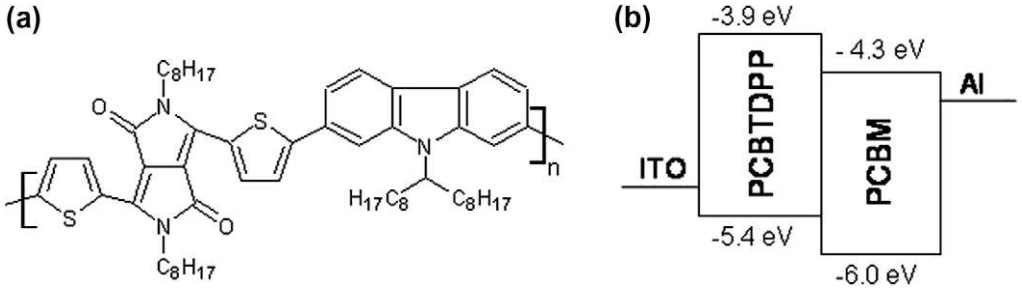

Scheme 1. (a) Chemical structure of PCBTDPP. (b) Energy band diagram of the BHJ solar cell (PCBTDPP: PCBM).

strates increased EQE across the whole visible spectral range, with a maximum of 45% at 450 nm, which indicates that the $PC_{70}BM$ is a much better acceptor than $PC_{60}BM$ for use with PCBTDPP. All the following optimizations will be done with this acceptor.

In order to optimize the ratio, thickness, and morphology of PCBTDPP:$PC_{70}BM$ bulk heterojunction films and study their effects on the device performance, solar cells using this couple with different weight ratios (1:2, 1:3, 1:4), thicknesses (from 60 to 130 nm) were fabricated with different organic solvents, and tested using standard solar cell characterization procedures.

First, we tested the effect of the PCBTDPP:$PC_{70}BM$ ratio on the device performance (Table 1). With increasing $PC_{70}BM$ ratio, the open-circuit voltage remained the same for all devices, but the short-circuit current density increased from 6.7 mA/cm^2 to 7.9 mA/cm^2 when the ratio was increased from 1:2 to 1:3. It is known that higher acceptor ratio ($PC_{60}BM$ or $PC_{70}BM$) favours the formation of a phase separated interpenetrated network with sizable domains [13], which in turn favours effective charge separation. However, the current decreased again to 6.5 mA/cm^2 when the ratio was increased up to 1:4. The impact of the donor ratio on the fill factor is also obvious. The maximum value was obtained with a ratio of 1:3. It is clear that the concentration of $PC_{70}BM$ in the blend has a strong impact on J_{sc} and the FF. For the PCBTDPP:$PC_{70}BM$ system, the best ratio is 1:3. Too high a $PC_{70}BM$ ratio will not only lead to lower J_{sc} and fill factor, but also a lower V_{oc}. Janssen et al. have already shown that saturating the active layer with $PC_{70}BM$ leads to a decrease in the J_{sc} and fill factor due to phase separation [14].

Table 1
Best performance parameters of BJH solar cell with PCBTDPP:$PC_{70}BM$ composites of different weight ratios under AM1.5G illumination of 100 mW cm^{-2}.

(PCBTDPP:$PC_{70}BM$)	J_{sc} (mA/cm^2)	V_{oc} (V)	FF (%)	η (%)
1:2	6.7	0.8	41	2.2
1:3	7.9	0.8	47	3.0
1:4	6.5	0.8	40	2.0

Table 2
Performance parameters of PCBTDPP:$PC_{70}BM$ (1:3) BJH solar cells of different thicknesses made with different solvents under AM1.5G irradiation of 100 mW cm^{-2}.

Active layers solvents	Thickness (nm)	J_{sc} (mA/cm^3)	V_{oc} (V)	FF (%)	η (%)
$CHCl_3$	70	2.2	0.74	45	0.7
	83	3.7	0.73	35	0.9
	90	4.8	0.72	35	1.2
	110	2.8	0.73	40	0.8
CB	80	6.2	0.79	48	2.3
	90	6.8	0.79	47	2.5
	100	5.2	1.79	46	1.9
	110	4.6	1.79	46	1.7
ODCB	74	7.7	0.80	46	2.8
	90	8.6	0.80	47	3.2
	105	8.1	080	45	2.9
	130	7.8	0.80	42	2.6

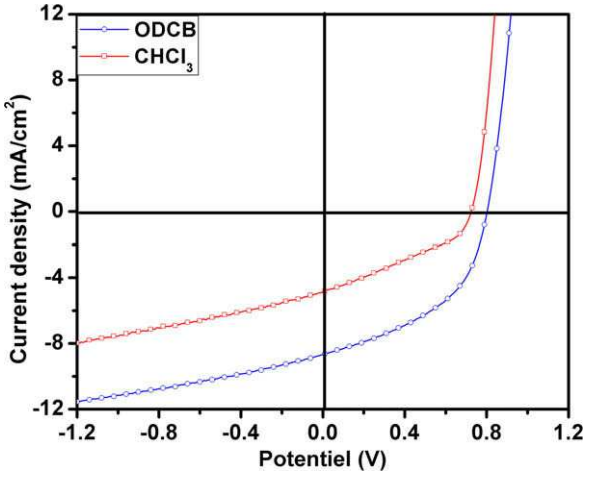

Fig. 3. *J–V* characteristics of ITO/PEDOT:PSS/PCBTDPP:3$PC_{70}BM$/LiF/Al devices with an active layer prepared by using $CHCl_3$ or ODCB as solvent. The active layers have the same thickness of 90 nm.

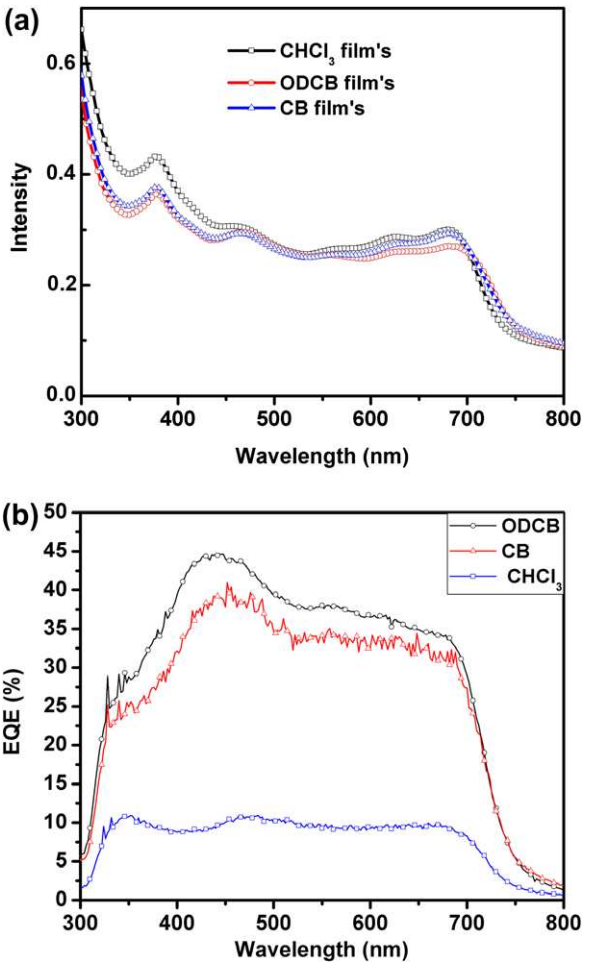

Fig. 4. (a) UV–vis absorption of PCBTDPP:$PC_{70}BM$ films prepared using different solvents; (b) External quantum efficiency (EQE) spectra of corresponding PCBTDPP:$PC_{70}BM$ solar cells.

The choice of electron donor and acceptor materials for use in BJH devices and their loading ratio is the first important step towards solar cell optimization. The choice of solvents is another important step [15]. It has a strong impact on the nano-scale morphology of the active layer, which plays an important role in the performance of solar cells [16] and OFETs [17].

In order to study the solvents effect on the morphology of the active layer and the solar cell performance, thin films of PCBTDPP:PCBM (1:3) blend were prepared using non-aromatic and aromatic solvents.

Table 2 summarizes the photocurrent densities of the solar cells in which the active layers were prepared with different solvents. Non-aromatic (chloroform ($CHCl_3$)) and aromatic (chlorobenzene (CB), and 1,2-Orthodichlorobenzene (ODCB)) solvents were used to study the solvent effect. Different active layer thicknesses were realised by using different spin rate in order to study the thickness effect on the photovoltaic performance of these devices.

The best device prepared using chloroform as solvent has a power conversion efficiency $\eta = 1.2\%$, a short-circuit current density $J_{sc} = 4.8$ mA/cm^2, an open-circuit voltage $V_{oc} = 0.72$, and a fill factor FF = 35%. The devices prepared using chlorobenzene as solvent show higher performance with $\eta = 2.5\%$, $J_{sc} = 6.8$ mA/cm^2, $V_{oc} = 0.79$ Volt, and FF = 47%. The devices prepared by using ODCB as solvent demonstrate the best performance with $\eta = 3.2\%$, $J_{sc} = 8.6$ mA/cm^2, $V_{oc} = 0.80$ V, and FF = 47%. The I–V curves of devices prepared using $CHCl_3$, and ODCB are shown in Fig. 3. Through this device optimization process, our PCBTDPP based solar cells have improved ~100% in power conversion efficiency as compared to our initial result 1.6%

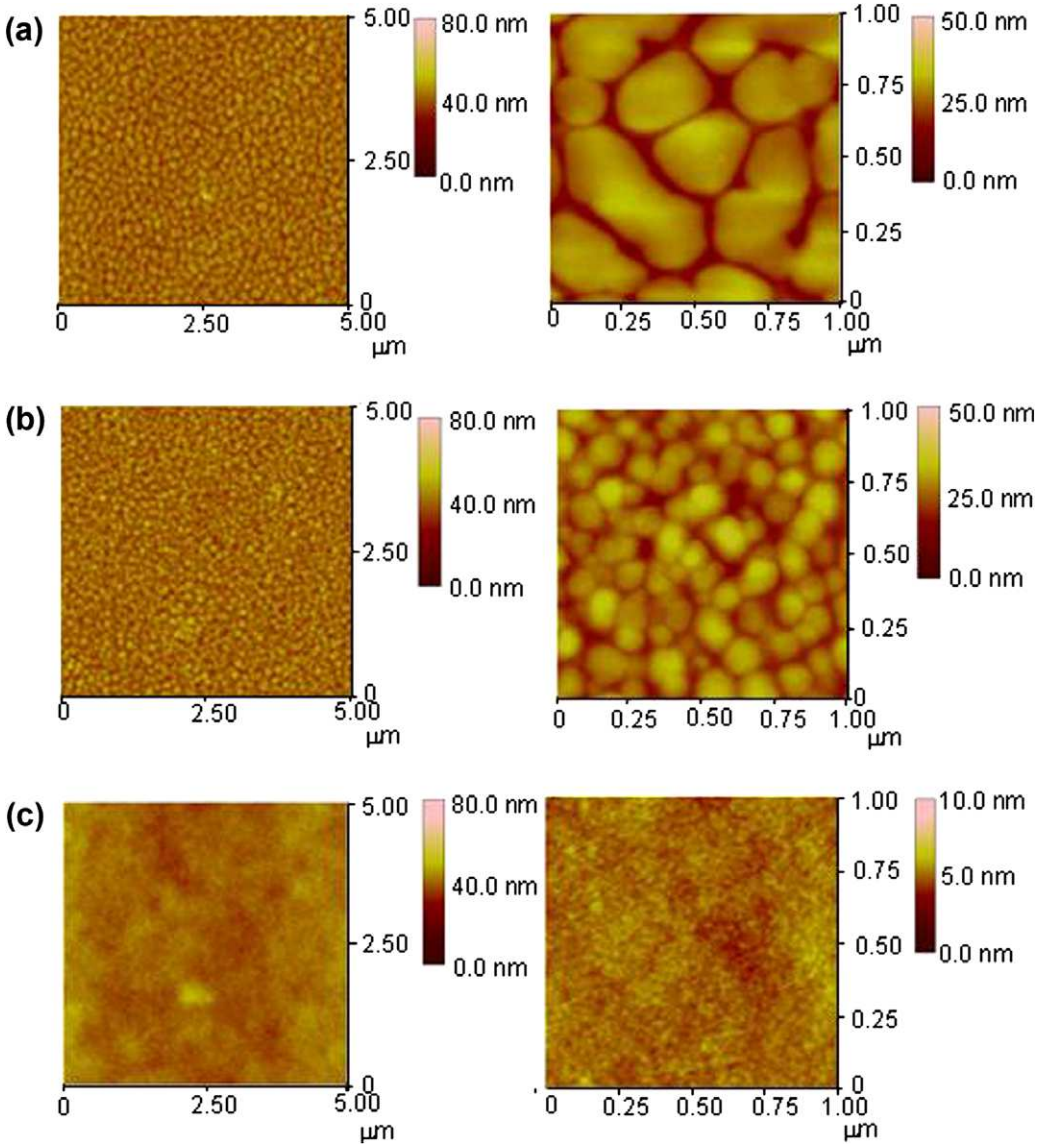

Fig. 5. 5×5 µm and 1×1 µm AFM images of PCBTDPP:3PC$_{70}$BM blend films spin-cast from different solvents: $CHCl_3$ (a), CB (b), and ODCB (c). These pictures are taken from active layers of the best devices obtained for each solvent.

[11], and ~40% as compared to the results reported recently by Zhou et al. (2.26%) using a similar polymer with different side chain [12]. This improvement can be attributed to the increased light absorption by replacing $PC_{60}BM$ with $PC_{70}BM$, as well as the optimized donor/acceptor ratio and active layer thickness.

The best values of the fill factor up to 45% were obtained when aromatic solvent (ODCB or chlorobenzene) was used, and the fill factor remains reasonably high up to an active layer thickness of 130 nm. In contrast, when chloroform was used as solvent, the average FF is less than 40%. The best values of short-circuit current were obtained at an active layer thickness of 90 nm in each case, independent of the solvent choice. The best V_{oc} values were obtained when chlorobenzene or ODCB was used as solvent. The V_{oc} decreased dramatically when chloroform was used, the same as other photovoltaic parameters, indicating that non-aromatic solvent is not preferred for making PCBTDPP based devices.

From the data shown in Table 2, we can conclude that for PCBTDPP:$PC_{70}BM$ (1:3) devices, the best film thickness is around 90 nm for maximum efficiency, and ODCB is preferred for active layer preparation.

The better performance of the devices prepared by ODCB is attributed to the optimized nano-scale morphology of the bulk heterojunction film with an average domain size around 20 nm. The most noticeable improvements in device performance are the fill factor and short-circuit current density, which are known as parameters directly dependant on the nano-scale morphology.

The external quantum efficiency (EQE) of a photovoltaic cell is given by the ratio between the number of electrons produced in the outer circuit and that of incident photons on the device. Fig. 4 compares the EQE spectra of PCBTDPP:$PC_{70}BM$ solar cells prepared with different solvents, as discussed above. The device prepared using ODCB as solvent shows the best overall EQE, which has the slowest drying rate among the three. The highest monochromatic EQE values for devices prepared using ODCB or CB are 44% and 41%, respectively. While that of the device prepared using chloroform is less than 22%. These results confirmed that even if we optimize the acceptor and donor ratio and the active layer thickness, it is also necessary to use the right solvent for the active layer preparation.

The surface morphology of PCBTDPP:$PC_{70}BM$ (1:3) active layers prepared using the three solvents was investigated by the atomic force microscopy (AFM). The tapping mode AFM images of the film prepared using chloroform (Fig. 5) show over-sized grain structures ~140 nm, indicating a large scale phase separation. The domains size is too large for efficient exciton dissociation. The surface morphology of the film spin cast from chlorobenzene is well-defined and the domain size is much smaller, ~50 nm. The situation improves even further when 1.2-dichlorobenzene is used as solvent, the film show much finer grain sizes (20–30 nm) with better organization and uniformity. This best organization observed on AFM pictures is in agreement with the solar cell performance. This indicates that the choice of solvent for active layer preparation is a crucial factor to get the optimum film morphology in order to realize the best device performance [18,19].

3. Conclusion

In this work, we have demonstrated how to control the nano-scale morphology of PCBTDPP:$PC_{70}BM$ bulk heterojunction by choosing right solvent, and donor/acceptor ratio. For this particular material, aromatic solvents deliver better device performance. AFM study connects the high device performance to better and organized phase-separated domains which provides an optimized *D–A* interface for efficient exciton dissociation and continuous electron and hole conducting channels necessary for efficient charge transport between electrodes. By replacing $PC_{60}BM$ with $PC_{70}BM$, we have significantly increased the light absorption in the spectral region where the PCBTDPP absorption is at minimum, and thus improved the short-circuit current density. With these optimization steps, we have improved the PCE from 1.6% in our previous study [11] to 3.2%.

Acknowledgments

This work was supported by the Sustainable Development Technology Canada (SDTC) program. The authors acknowledge Raluca Movileanu for the AFM measurements.

References

[1] G. Dennler, M.C. Scharber, C.J. Brabec, Polymer-fullerene bulk-heterojunction solar cells, Adv. Mater. 21 (2009) 1323–1338.
[2] S. Allard, M. Forster, B. Souharce, H. Thiem, U. Scherf, Organic semiconductors for solution-processable field-effect transistors (OFETs), Angew. Chem., Int. Ed. 47 (2008) 4070–4098.
[3] S.W. Thomas, G.D. Joly, T.M. Swager, Chemical sensors based on amplifying fluorescent conjugated polymers, Chem. Rev. 107 (2007) 1339–1386.
[4] R.B. Aïch, N. Blouin, A. Bouchard, M. Leclerc, Electrical and thermoelectric properties of poly(2,7-carbazole) derivatives, Chem. Mater. 21 (2009) 751–757.
[5] J. Roncali, Molecular engineering of the band gap of π-conjugated systems: facing technological applications, Macromol. Rapid Commun. 28 (2007) 176–1775.
[6] E. Bundgaard, F.C. Krebs, Low band gap polymers for organic photovoltaics, Sol. Energy Mater. Sol. Cells 91 (2007) 954–985.
[7] S.H. Park, A. Roy, S. Beaupre, S. Cho, N. Coates, J.S. Moon, D. Moses, M. Leclerc, K. Lee, A.J. Heeger, Bulk heterojunction solar cells with internal quantum efficiency approaching 100%, Nat. Photonics 3 (2009) 297–302.
[8] N. Blouin, A. Michaud, D. Gendron, S. Wakim, E. Blair, R.N. Plesu, M. Bellette, G. Durocher, Y. Tao, M. Leclerc, Toward a rational design of poly(2,7-carbazole) derivatives for solar cells, J. Am. Chem. Soc. 130 (2008) 732–742.
[9] L. Burgi, M. Trubiez, R. Pfeiffer, F. Bienewald, H.J. Kirner, C. Winnewisser, High-mobility ambipolar near-infrared light-emitting polymer field-effect transistors, Adv. Mater. 20 (2008) 2217–2224.
[10] Y. Zou, D. Gendron, R. Neagu-Plesu, M. Leclerc, Synthesis and characterization of new low-bandgap diketopyrrolopyrrole-based copolymers, Macromolecules 42 (2009) 6361–6365.
[11] Y.P. Zou, D. Gendron, R.B. Aïch, A. Najari, Y. Tao, M. Leclerc, A high-mobility low-bandgap poly(2,7-carbazole) derivative for photovoltaic applications, Macromolecules 42 (2009) 2891–2894.
[12] E. Zhou, S. Yamakawa, K. Tajima, C. Yang, K. Hashimoto, Synthesis and photovoltaic properties of diketopyrrolopyrrole-based donor−acceptor copolymers, Chem. Mater. 21 (2009) 4055–4061.
[13] S. ALem, R. Bettignies, J.-M. Nunzi, M. Cariou, Efficient polymer-based Interpenetrated network photovoltaic cells, Appl. Phys. Lett. 12 (2004) 2178–2180.
[14] J.K.J. van Duren, X. Yang, J. Loos, C.W.T. Bulle-Lieuwma, A.B. Sieval, J.C. Hummelen, J.R.A. Janssen, Relating the morphology of poly(p-phenylene vinylene)/methanofullerene blends to solar-cell performance, Adv. Funct. Mater. 14 (2004) 425–434.

[15] S. Barrau, V. Andersson, F. Zhang, S. Masich, J. Bijleveld, M.R. Andersson, O. Inganäs, Nanomorphology of bulk heterojunction organic solar cells in 2D and 3D correlated to photovoltaic performance, Macromolecules 42 (2009) 4646–4650.
[16] F. Zhang, K.G. Jespersen, C. Björström, M. Svensson, M.R. Andersson, V. Sundström, K. Magnusson, E. Moons, A. Yartsev, O. Inganäs, Influence of solvent mixing on the morphology and performance of solar cells based on polyfluorene copolymer/fullerene blends, Adv. Funct. Mater. 16 (2006) 667–674.
[17] Z. Bao, A. Dodabalapur, A-J. Lovinger, Soluble and processable regioregular poly(3-hexylthiophene) for thin film field-effect transistor applications with high mobility, Appl. Phys. Lett. 69 (1996) 4108–4110.
[18] J.F. Chang, B. Sun, D.W. Breiby, M.M. Nielsen, T.I. Solling, M. Giles, L. McCulluch, H. Sirringhaus, Enhanced mobility of poly(3-hexylthiophene) transistors by spin-coating from high-boiling-point solvents, Chem. Mater. 16 (2004) 4772–4776.
[19] L.M. Chen, Z. Hong, G. Li, Y. Yang, Recent progress in polymer solar cells: manipulation of polymer: fullerene morphology and the formation of efficient inverted polymer solar cells, Adv. Mater. 21 (2009) 1434–1449.